Design Exploration of a Mild Hybrid Electrified Aircraft Propulsion Concept

Zachary J. Frederick*, Thomas J. Hallock†, and Thomas A. Ozoroski‡
NASA Langley Research Center, Hampton, VA, 23681

Jeffryes W. Chapman§ and Caroline A. Kuhnle¶
NASA Glenn Research Center, Cleveland, OH, 44135

Peter C. Frederic‖
Tecolote Research, Inc., Santa Barbara, CA, 93111

NASA has performed in-depth research and analysis into hybrid-electric aircraft concepts featuring high levels of electrification. Many of these concepts were found to be infeasible, whereas feasible designs were significantly heavier and more costly compared to conventional concepts. This study presents the development and analysis of an alternative mild hybrid concept that uses relatively low levels of stored electric energy applied strategically throughout the mission. The team researched several mild hybrid technologies, developed integrated aircraft models, and then evaluated the effects of these technologies on vehicle level performance metrics. Technologies explored in this study include the Turbine Electrified Energy Management system, electric taxi, electric climb assist, and replacing the auxiliary power unit with on-board electric energy storage. Key enabling technologies were energy storage devices that prioritized high power output over energy capacity and integrating electric motors with the shafts of the gas turbine engines. Significant performance improvements were observed when applying multiple technologies separately and in combination, with the most promising configuration incorporating all of them at once. Results for the mild hybrid configuration indicate an 8.2% reduction in block fuel, a 7.7% reduction in equivalent CO_2 emissions, and a 3.5% increase in gross takeoff weight compared to a conventional baseline. Results of a cost analysis suggest the mild hybrid slightly reduces direct operating cost plus interest, which demonstrates that aircraft emissions can be significantly reduced without the cost increases associated with highly electrified concepts.

Nomenclature

E_{req}	=	energy required
m	=	mass of a component of the energy storage system
$P_{climb\ assist}$	=	climb assist power
$P_{req,cont}$	=	continuous power required
$P_{req,peak}$	=	peak power required
SE	=	energy content per unit mass
SP_{cont}	=	continuous power output per unit mass
SP_{peak}	=	peak power output per unit mass
W_{ESS}	=	energy storage system weight
$W_{powertrain}$	=	electric powertrain weight
η_{TEEM}	=	efficiency boost due to Turbine Electrified Energy Management

*Aerospace Engineer, Aeronautics Systems Analysis Branch, 1 N. Dryden Street, MS 442, Hampton, VA, Member
†Aerospace Engineer, Analytical Mechanics Associates, 21 Enterprise Parkway, Suite 300, Hampton, VA
‡Aerospace Engineer, Analytical Mechanics Associates, 21 Enterprise Parkway, Suite 300, Hampton, VA, Member
§Aerospace Engineer, Propulsion Systems Analysis Branch, 21000 Brookpark Road, MS 5-11, Cleveland, OH
¶Aerospace Engineer, Propulsion Systems Analysis Branch, 21000 Brookpark Road, MS 5-11, Cleveland, OH, Member
‖Cost Analyst, 5383 Hollister Ave., Suite 100, Santa Barbara, CA

I. Introduction

NASA's Advanced Air Transport Technology (AATT) project has performed extensive research into hybrid-electric aircraft concepts in recent years with the goal of reducing fuel consumption and emissions. The majority of these concepts have featured high levels of hybridization with a significant proportion of the energy to complete the mission coming from electric sources rather than from burning hydrocarbon fuels. One challenge with this approach is that the specific energy (SE) of electric energy storage devices is vastly inferior to jet fuel. The energy content of jet fuel is approximately 43 MJ/kg [1]. Assuming a thermodynamic efficiency of 55% for combustion in a gas turbine engine, this yields a SE of around 6500 Wh/kg for jet fuel. For reference, state-of-the-art (SOA) batteries, assuming 90% transmission efficiency, have pack-level SEs around 135 Wh/kg [2]. Given those physical and chemical realities, the SE of jet fuel is nearly fifty times greater than that of SOA batteries. Replacing a large portion of the energy contained in jet fuel with batteries requires battery weights which result in large increases in aircraft empty weight and acquisition cost, as well as degraded design feasibility. Without dramatic improvements in battery SE, directly offsetting fuel with batteries will remain a serious challenge.

An alternative hybrid-electric architecture termed a "mild hybrid" relies on relatively small energy storage devices that supply supplementary electric power strategically throughout the mission. One application of this approach is peak power shaving, where electric power is applied during transient peaks in the vehicle power requirement at specific flight conditions such as rolling takeoff or top-of-climb. This reduces the peak power that the gas turbine must be sized to produce, which allows it to be optimally designed for the steady-state operating point resulting in an overall increase in system efficiency. This efficiency benefit, combined with only modest increases in empty weight due to the addition of batteries and electric motors, has the potential for significant vehicle level benefits. Since electric energy storage requirements for this approach are low, battery weights remain relatively small even assuming current-day energy storage technology. This makes a mild hybrid architecture more realizable in the near-term than concepts with higher levels of hybridization.

Section II describes the modeling approach for the aircraft sizing and mission analysis, each of the mild hybrid technologies, and the cost analysis. Section III details trade study results from applying different combinations of technologies and modeling assumptions. Section IV summarizes the results and details future work.

II. Approach

This paper explores technologies most compatible with a mild hybrid approach to electrified aircraft propulsion (EAP). The key technologies investigated were the energy storage system (ESS), the Turbine Electrified Energy Management (TEEM) system [3], electric taxi (E-taxi), electric climb assist, and replacing the auxiliary power unit (APU) with the on-board ESS. Modeling techniques were developed for each technology, and then combinations of technologies were applied with the goal of maximizing vehicle level benefits (e.g., reductions in block fuel and life cycle equivalent CO_2 emissions (CO_2e)). The parameter CO_2e represents the total global warming impact of all the emissions produced from operating the aircraft, calculated as an equivalent amount of CO_2. This includes emissions from extracting, processing, and burning fuel as well as the emissions from producing electricity. The same approach for computing CO_2e was used as in the study by Marien et al. [4], which assumed 3.7625 lb_m of CO_2e per pound of fuel consumed and 200 g of CO_2e per kWh of electricity produced, representing a U.S. electricity grid with most coal-powered electricity generation phased out.

A. Aircraft Sizing and Mission Analysis

The team selected an advanced tube and wing, single-aisle, 154 passenger class configuration with an assumed entry into service (EIS) of 2035 as a baseline for comparison. The analysis framework shown in Fig. 1 is built within ModelCenter®*, a multidisciplinary analysis tool which allows several disciplinary codes to be integrated in one comprehensive model. The integrated analysis model uses the Flight Optimization System (FLOPS) [5] for aircraft sizing and mission analysis and OpenVSP [6] for geometry modeling. Within FLOPS, the aircraft is sized for two missions: a 3500 NM design mission and a 900 NM economic mission, which is representative of a typical mission length, both cruising at Mach 0.8. Figures of merit such as reduction in block fuel are typically referenced to the economic mission. For the propulsion system, the Numerical Propulsion System Simulation (NPSS) [7] is used to perform the thermodynamic cycle analysis of the gas turbine engine. The results of this analysis is then used to produce FLOPS-readable engine decks (tables of gross thrust, ram drag, fuel flow rate, and electric power insertion for different

*https://www.phoenix-int.com/product/modelcenter-integrate/

Mach, altitude, and throttle settings).

A simple convergence loop is used to enforce several constraints on the design. The overall engine size is scaled by a single "thrust" term which is taken as sea level static gross thrust, and the overall wing geometry is scaled by a single "wing area" term, with wingspan held constant since this class of aircraft is span constrained due to gate restrictions. These two design variables, thrust and wing area, are varied in order to satisfy two constraints: a fixed thrust loading, T/W, and a fixed wing loading, W/S. These two parameters are held fixed between configurations because they correlate loosely with takeoff and landing characteristics, and it was desirable for takeoff and landing performance to be similar across all configurations.

The "Optimize ESS" component in the model, as shown in Fig. 1, takes the energy and power requirements from the mission analysis and uses an optimizer to size the ESS to meet those requirements while minimizing the total weight of the system. This optimization problem is formulated as shown in Eq. (1). The convergence loop, shown in Fig. 1 by the orange "Solver" box, iterates until the ESS weight assumed in the aircraft sizing and mission analysis, W_{ESS}, and the weight calculated by the "Optimize ESS" component converge.

$$
\begin{aligned}
\min_{m_i, m_{i+1}, \ldots m_N} \quad & \sum_{i=1}^{N} m_i \\
\text{subject to} \quad & E_{req} - \sum_{i=1}^{N} m_i(\mathrm{SE}_i) \leq 0 \\
& P_{req,peak} - \sum_{i=1}^{N} m_i(\mathrm{SP}_{peak,i}) \leq 0 \\
& P_{req,cont} - \sum_{i=1}^{N} m_i(\mathrm{SP}_{cont,i}) \leq 0
\end{aligned}
\tag{1}
$$

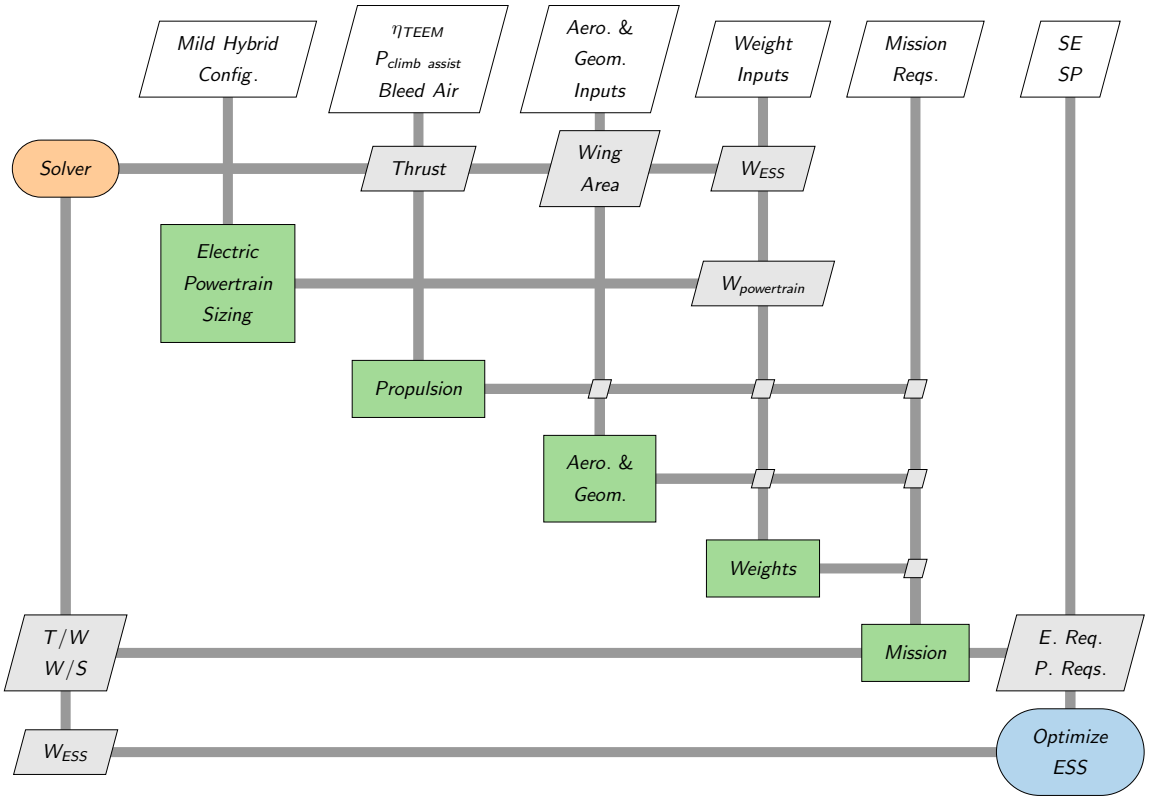

Fig. 1 Notional eXtended Design Structure Matrix (XDSM) representing the ModelCenter model.

B. TEEM Modeling

NASA Glenn Research Center's TEEM technology is the primary feature of the mild hybrid EAP concept. TEEM is a control technology for improving the transient operability of turbomachinery by modifying the engine's dynamic response [3]. The TEEM system works by using electric motors integrated into the high pressure shaft (HPS) and the low pressure shaft (LPS) of the gas turbine engine for power insertion and extraction. During transient power conditions, electric power can be inserted or extracted in order to more closely maintain steady-state conditions for the turbomachinery. To benefit from TEEM, the gas turbine must be redesigned as a coupled system with integrated electric motors, with an overall fuel efficiency benefit coming from a reduction in stall margin.

Quantifying the efficiency benefit due to TEEM is an area of active research, requiring turbomachinery redesign beyond the scope of this effort. Instead, the team performed a parametric trade of an assumed TEEM efficiency benefit from 0 to 3% with the goal of finding the "break-even" efficiency for TEEM to provide a block fuel benefit. If the break-even efficiency is outside the realistic range, then TEEM as a concept is not worth pursuing. The efficiency benefit was modeled as a uniform reduction in thrust specific fuel consumption (TSFC) across the engine deck.

From a dynamic engine analysis, we estimated that a 300 kW and a 400 kW electric motor would be required on the HPS and LPS, respectively, in order to implement TEEM. An electric powertrain was modeled for each motor including an inverter, DC-DC converter, circuit protection, cabling, and a thermal management system (TMS). The electric powertrain weight was estimated using assumed specific powers (SPs) for each component with the total EAP component weight added to the vehicle. The weight of the gas turbine engine was modeled in WATE++ [8]. The reduction in stall margin due to TEEM resulted in a slight reduction in engine weight. Because the transients that TEEM seeks to alleviate are infrequent and of a short 5 to 10 second duration, the total energy requirement is relatively small. Based on the upper bound, 6.12 MJ energy estimate provided in Kratz et al. [3] for TEEM during a 1.5 hour mission, we estimated 36 MJ of electric energy would be required for the 8 hour, 3500 NM design mission, and this requirement was passed to the ESS sizing component.

TEEM is the key enabling technology for the mild hybrid architecture. Integrating electric motors with the spools of the gas turbine allows expanded power extraction and injection beyond what is possible with a traditional engine. This approach enables new opportunities for electrifying the mission such as electric climb assist and in-flight recharging.

C. Replacing the APU with Energy Storage System

The primary function of an APU is to provide customer bleed air and electric power for the aircraft during ground operations, as well as to serve as an additional emergency power source in case the aircraft's main generators fail. The APU is useful for air starting the main engines as well as powering important subsystems like air conditioning and electric power at the gate, especially for airports that lack the necessary ground infrastructure. However, since the APU is normally off during flight, it is effectively 1,000 lb of dead weight during flight, making it a suitable target for weight reduction.

We assumed no-bleed air systems, which replace pneumatic subsystems powered by customer bleed air with electric-powered equivalents, would be ubiquitous by a 2035 EIS and incorporated them into both the conventional baseline and mild hybrid configurations. For no-bleed aircraft, the role of the APU is greatly diminished. Since the customer bleed air requirement is eliminated, during typical operation the APU provides electric power only during the narrow timespan when the main engines are off and the aircraft is away from airport electric power equipment and infrastructure. This study investigated replacing the APU entirely by adopting a no-bleed air system and using the ESS to provide electric power in place of the APU. An important caveat to this approach is that airport electric power becomes a requirement, both for recharging the ESS between flights and for supplying APU-equivalent power at the gate. The emergency power supply function of the APU was considered, with the ESS taking the place of the APU as an emergency power source; however, we did not quantify the time duration that emergency power would be required and simply assumed that the energy capacity of the ESS would be sufficient for an emergency diversion.

To model the no-bleed and no-APU case, we first estimated the power and energy requirements for the APU using airport planning documentation [9]. These power and energy requirements were then added to the sizing requirements for the ESS. The APU weight was removed, and the aircraft sizing and mission analysis was performed again. The trade we investigated was whether additional ESS weight required to perform the functions of the APU would be less than the weight of the APU, which would provide a net weight reduction and performance benefit for the aircraft.

D. E-taxi Model

The fuel consumed for taxi operations can be a relatively significant component of mission block fuel, especially for short range missions. The standard use of aircraft main engines to propel the aircraft is inefficient, with the engines typically producing more thrust at their idle condition than is necessary to move the aircraft around the taxiway [10, 11]. Also, the engines themselves operate inefficiently at idle, releasing extensive amounts of CO_2e into the air due to incomplete idle combustion [11]. Although single-engine taxiing may reduce fuel consumed by the aircraft during ground operations, it has a greater risk of foreign object debris due to the higher thrust levels required and is not recommended for runways with uphill slopes or slippery surfaces [12]. Alternatively, an E-taxi system could be tailored to specifically perform a taxi mission and have no emissions due to combustion.

In 2015, there were approximately 32 million flights with main-engine-operated taxi segments averaging 4 NM, resulting in 128 million NM of taxi operations occurring annually [13]. Aviation accounts for approximately 2% of worldwide CO_2 emissions, and airport carbon footprint accreditation found that 5 to 20% of all aviation emissions are due to aircraft ground operations [10], meaning electrifying ground operations has the potential to significantly reduce global CO_2 emissions. This is with the important caveat that the electric energy used for E-taxi is generated from renewable sources.

The mild hybrid E-taxi model is a modified version of the method developed by Nihad E. Daidzic [13], which approximates a simplified taxi mission as a series of constant velocity and constant acceleration segments. From this taxi model, the energy, power requirements, and fuel consumption can then be calculated. The taxi model includes a 17 minute taxi-out mission with four acceleration and braking segments and a 9 minute taxi-in with two acceleration and braking segments. Idle times were added to ensure taxi duration matched the average at four major U.S. airports: ATL, BOS, IAD, and LAX. These data were sourced using the Aviation System Performance Metrics (ASPM) tool [14]. A subset of these data over a representative timespan for taxi-out and taxi-in is shown in Tables 1 and 2, respectively.

Table 1 ASPM: Taxi Times Standard Report - Departures

Facility	Number of Departures	Average Taxi Out Time, min	Departures with Taxi Out Time, min					
			<20	20-39	40-59	60-119	120-179	≥ 180
ATL	68,758	17.2	51,408	16,370	642	291	47	0
BOS	26,512	18.6	18,875	6,538	752	311	33	3
IAD	17,490	17.5	13,230	3,731	397	118	11	3
LAX	49,429	16.5	37,797	10,973	560	94	5	0
Total	162,189	17.2	121,310	37,612	2,351	814	96	6

From 01/2016 To 02/2016 ; Generated Tue Mar 21 09:29:54 EDT 2023

Table 2 ASPM: Taxi Times Standard Report - Arrivals

Facility	Number of Arrivals	Average Taxi In Time, min	Arrivals with Taxi In Time, min					
			<15	15-29	30-44	45-59	60-74	≥ 75
ATL	68,612	8.32	64,538	3,694	311	45	16	8
BOS	26,290	7.07	25,416	654	111	49	23	37
IAD	17,455	6.39	17,283	160	5	5	0	2
LAX	49,205	12.3	38,302	8,560	1,744	419	121	59
Total	161,562	9.12	145,539	13,068	2,171	518	160	106

From 01/2016 To 02/2016 ; Generated Tue Mar 21 09:29:54 EDT 2023

1. Taxiway Parameters and Conditions

Each taxi segment had a headwind ranging from 10 to 30 knots and an inclination ranging from 0% to +1.5%, which is the maximum taxi slope allowed by the International Civil Aviation Organization (ICAO) [11]. Both of these

parameters were fixed for each segment of constant acceleration and constant velocity. This allowed the team to calculate the peak power and maximum torque required if the aircraft must accelerate in strong winds or up such an incline. Much like other E-taxi studies [13], crosswind and steering dynamics were deemed not to have a significant effect on taxi behavior and were deemed out of the scope for this study by the team. A wet surface coefficient of 0.5 was used to ensure the wheels never exceeded the maximum torque value that would result in wheel slip, for both acceleration and braking phases. Other relevant coefficients involved in the force calculations in the E-taxi model were a roll inertia of 1.01 [13], a coefficient of rolling friction for airplane tires of 0.02 [15], and an additional landing gear drag coefficient of 0.001 [16].

The required rate of acceleration had a significant effect on the overall energy required for E-taxi. Other taxi models have based their maximum acceleration of 0.15 m/s^2 [12] and 0.25 m/s^2 [11] on a requirement set by ICAO to meet a minimum acceleration for crossing an active runway. These studies sought to minimize the overall power required by the E-taxi system at the cost of lowering the acceleration rate far below typical aircraft behavior, which raises the concern of delays due to slow movement on the tarmac. The main justification for keeping the power requirement low in these studies was because the intent was to power the E-taxi system with the APU [11, 13] or with a combination of the APU and fuel cells [12]. The APU of a single-aisle aircraft was estimated to provide about 173 kW [9], which is far lower than the 800 kW peak power output of the ESS in the mild hybrid, which is sized by simultaneous operation of both 400 kW LPS motors required for TEEM. This makes the mild hybrid much less constrained by peak power, and the final acceleration value chosen in this study can easily be changed to meet energy constraints or new E-taxi regulations. The model by Daidzic [13] had a maximum acceleration of 1.03 m/s^2, based on typical aircraft taxi behavior, which the team found to raise power and motor torque requirements unnecessarily high. Thus the maximum acceleration capabilities of the mild hybrid was set to a rate of 0.65 m/s^2.

2. Propulsive Method

The prospect of operating the gas turbine engines electrically with the TEEM motors was investigated, but the overall propulsive efficiency was found to be less than 10%, since the aircraft main engines operate in a non-optimum thrust range during ground operations [17]. Relying on ground vehicles to tow the aircraft during taxi was considered, but we decided maintaining the aircraft's ability to taxi unassisted was more desirable. External pushback operations have been identified as the largest contributing factor slowing down the total ground procedure [17]. The introduction of taxi-assist vehicles would greatly increase the complexity of ground operations.

Therefore, we elected to perform E-taxi using electric motors embedded in the wheels with electric energy provided by an ESS. Since only 6% to 10% of the weight of the aircraft is supported by the nose gear, the best arrangement is to place electric motors in the main gear wheels to maximize traction [13]. These high-torque motors installed in the landing gear have been used in multiple studies [13, 17] featuring single-aisle aircraft with electrified ground operations. Motors within the wheels could also be used for pre-rotating tires before touching down on landing in order to reduce wear, as well as regenerative braking [13] to recapture some of the kinetic energy of the aircraft as electric energy. In addition to intense use upon landing, aircraft disc brakes are employed constantly during taxi operations when the aircraft main engines are used as the method of propulsion, since the idle thrust produced is greater than is typically required for taxi. The implementation of these motors, along with no longer using flight engines for E-taxi, will reduce the wear and greatly extend the lifetime of the disc brakes [11, 17].

The gas turbine engines were kept completely off during taxi operations except for a required 180 second period of warm-up time for taxi out and a 180 second idle cool-down period for taxi in. Thus, the tail end of taxi-out and the initial segment of taxi-in can be operated using idle engine thrust, since the engines must be operated on idle to warm or cool [11]. Therefore, with our E-taxi concept of operations (ConOps), there is some fuel consumption, but by making use of the idle thrust generated during engine warm-up and cool-down, we can lower the energy requirement for the rest of E-taxi.

3. Regenerative Braking and In-Flight Recharging

The use of electric motors and an ESS enables the kinetic energy of a moving vehicle to be recaptured. For current electric cars operating in an urban environment, regenerative braking is one of the most significant contributors to energy efficiency [18], with SOA systems able to recover about 65% of the kinetic energy while braking [19]. Regenerative braking was applied to all stopping portions of taxi-in and taxi-out at a g-force of one-tenth of a g (0.98 m/s^2), but since the aircraft is traveling at a relatively low speed, the savings from all segments was less than 1 MJ (less than 1% the total energy required for E-taxi).

The best application of regenerative braking was upon landing, which involved slowing the aircraft from a touchdown speed of approximately 74 m/s to a nominal taxi speed. This allows for the application of the maximum torque of the electric motors in the wheels to be applied for about 25 seconds while the standard disc brakes are used to aid in slowing the aircraft. The force produced by the motors and energy uptake in the battery is sized with respect to the peak acceleration segment for E-taxi, so the energy capable of being recovered will change with motor size. The total energy regained upon landing is 11 MJ, or about 8.5% of the energy required for taxi-in. It is advised that a study be done on the effect of short-duration, high-power charging of batteries; however, if the aircraft uses a high-power ESS such as a supercapacitor or flywheel coupled with a battery, then the burst can be distributed over time to the battery without additional risk of wear.

Rather than carry additional ESS weight needed for taxi-in as dead weight throughout the entire flight, we considered recharging the ESS using the integrated TEEM motors and operating the gas turbine engines as power generators during the descent phase of flight. This meant operating the engines at a slightly higher power output than what was required during descent and directing this power towards the ESS to store the energy required for taxi-in. The team found that the fuel consumed by raising the power output of the engines was several times higher than the approximately 16 lb of fuel consumed by carrying the 250 lb of additional ESS storing the taxi-in energy, so we elected to not adopt in-flight recharging as part of our ConOps.

4. Impact of Replacing APU with ESS on E-taxi

Replacing the APU with the ESS resulted in an additional sizing consideration. Initially, we sized the ESS to supply the APU-equivalent power and energy for an average taxi mission duration; however, we needed to quantify the impact of longer taxi missions which happen less frequently, but as can be seen in Tables 1 and 2, do occur. Our ConOps dictates that for a taxi mission longer than what the ESS was sized for, the aircraft should turn on its main engines and continue the taxi using engine thrust. Therefore, for these longer taxi missions, the aircraft is burning more fuel. An alternative strategy would be to size the ESS to accommodate a longer than average taxi mission, but for the majority of taxi missions this ESS would be oversized resulting in additional fuel burn incurred by carrying more weight. This represents a design trade with the goal of minimizing the total fuel burn of the entire fleet of aircraft performing a range of taxi missions. Using the data contained in Tables 1 and 2, we directly simulated the impact of varying the design taxi mission duration. This trade found that for a fleet of over 160,000 flights out of four large airports in the United States, adding an additional 360 lb of ESS weight minimized block fuel for the entire fleet by providing enough energy for 20 additional minutes of APU-equivalent power output.

E. Electric Climb Assist

The electric motors on the LPS, primarily used for TEEM, are available for power insertion during other mission segments. Electric power insertion was modeled in NPSS as added power to the LPS. Typically, either the rolling takeoff or the top-of-climb operating condition are the most constraining point for the gas turbine engine design. At top-of-climb, the engine is operating at its maximum throttle setting at a high altitude (and reduced air density). We modeled the addition of electric power during rolling takeoff and throughout climb, with the amount of climb assist power decreasing with altitude such that it is zero at cruise. By engaging the LPS electric motor during rolling takeoff and climb, less power is required from the gas turbine at rolling takeoff and top-of-climb. Relaxing these sizing constraints may allow the engine to be better optimized for fuel efficiency at its cruise condition. Since the majority of fuel consumption occurs at cruise, this application of electric power insertion would produce the largest benefit in terms of block fuel.

F. Energy Storage System

The high power and low energy capacity requirements for the mild hybrid ESS are unconventional compared to typical EAP concepts that feature greater levels of hybridization. The electrified flight operations such as TEEM, E-taxi, and climb assist require lots of power to be delivered over a range of seconds to a few minutes, with the total electric energy requirement remaining under 1% of the total energy required for the economic mission. The ESS was sized to satisfy the requirements in terms of energy, peak power, and continuous power for each respective mild hybrid configuration. The distinction between peak and continuous power requirements is an important one, since ESSs are typically rated to provide some power output continuously as well as a higher power for a short time duration (on the order of several seconds) without causing damage to the ESS. The energy and power requirements for the ESS for several different mission ConOps are shown in Table 3.

Table 3 Electric energy and electric power requirements for different mission ConOps

	Energy	Power Requirement, MW	
Mission ConOps	Requirement, MJ	Peak	Continuous
TEEM	36	0.80	0
E-taxi	120	0.72	0.27
Climb Assist	330	0.80	0.80
All	490	0.80	0.80

Batteries, supercapacitors, and flywheels were selected as the most promising components for meeting the energy storage requirements of a mild hybrid. They were arranged into various systems to store energy: a battery-only energy storage system (BESS), a flywheel energy storage system (FESS), and a hybrid energy storage system (HESS) with a battery coupled with either a supercapacitor or a flywheel. Since the pack-level SE and SP of future ESSs can only be estimated for an EIS of 2035, three values were assigned to each ESS based on conservative, nominal, and aggressive assumed improvements in energy storage technology. These assumptions are summarized in Tables 4 and 5. This strategy is the same as the one used in a study by Tiede et al. [20] which developed SE projections for future electrified aircraft.

Table 4 Pack-level specific energy assumptions

Technology Level	Battery, Wh/kg	Supercapacitor, Wh/kg	Flywheel, Wh/kg
Conservative	275	35	45
Nominal	350	60	150
Aggressive	500	125	280

Table 5 Pack-level specific power assumptions

	Battery, W/kg		Supercapacitor, W/kg		Flywheel, W/kg	
Technology Level	Peak	Continuous	Peak	Continuous	Peak	Continuous
Conservative	550	275	6,000	1,200	150	150
Nominal	700	350	8,000	1,600	500	500
Aggressive	1,000	500	10,000	2,000	970	970

For ESS SEs higher than the provided aggressive estimates in this study, there are diminishing returns on the block fuel saved by the mild hybrid concept. Since the ESS in the mild hybrid stores less than 1% of the total flight energy, ESS weight is not a large proportion of aircraft gross weight; therefore, changes in SE have a more limited impact on aircraft performance metrics such as block fuel. This is in contrast to a more fully electrified aircraft where ESS SE is a critical design factor [21]. Significant breakthroughs in energy storage technology (SE and SP) would be of limited benefit to a mild hybrid configuration but may provide substantial benefits to a more electrified aircraft.

1. Batteries

Batteries are the most accessible and historically reliable option for electric energy storage; however, battery lifespan and degraded performance over time is a challenge for their use with EAP. To avoid the electrochemical damage that occurs from either fully charging or fully discharging the battery, twenty percent of the energy capacity of the battery is held in reserve, with the battery operating within a 90% to 10% state of charge [22]. Lithium-ion batteries are the most commonly used rechargeable battery today, but alternative battery chemistries under development may offer substantial improvements in SE and SP. Due to the relatively low SP of batteries when compared to high-power units like supercapacitors or flywheels, the total system energy capacity typically must be oversized to meet peak power requirements [23].

A study by Tiede et al. [20] assessed the theoretical and present-day SE, cycle-life, and technological maturity for several emerging battery technologies, including but not limited to Li-ion, Na–S, Li–S, lead-acid, NiMH, and $LiCoO_2$. Some of these novel chemical batteries have extremely high theoretical SEs but have not yet been successfully demonstrated beyond a cell-level in a laboratory, nor proven that they are capable of multiple cycles [22]. Therefore, they require significant breakthroughs to be available by the EIS of 2035. Estimates for battery SP as a function of SE were informed by a study by Aravindan et al. [24] which showed battery SP in W/kg roughly twice the magnitude of battery SE in Wh/kg being within the feasible design space for several battery chemistries.

The projections for the conservative, nominal, and aggressive SE values used within this study were greatly influenced by Tiede et al. [20], along with several other publications on historical battery trends [22, 25]. The conservative estimates were approximated to be slightly above SOA characteristics, assuming a slow but steady development in technology. The nominal battery SE assumption of 350 Wh/kg for 2035 EIS was selected based on a 2021 joint assessment issued by the U.S. Department of Energy and NASA [2]. The ceiling of battery SE for the aggressive value was set to 500 Wh/kg. It is important to note that battery SE beyond 500 Wh/kg had diminishing returns in terms of block fuel benefit since ESS weight is not a large proportion of gross weight for a mild hybrid.

2. Supercapacitors

This study investigated supercapacitors, also known as ultracapacitors, as a way to provide the high amounts of power instead of an excessively heavy battery sized for power output. Advancements in supercapacitor technology in recent years, including the development of graphene-based electrodes, have made supercapacitors increasingly attractive as an ESS [26]. Projections of supercapacitor SE and SP were made according to the potential of graphene technology by the EIS of 2035 [22, 27]. From these studies, we estimated the range of plausible supercapacitor SEs between a conservative 35 Wh/kg and the aggressive maximum of 125 Wh/kg. We estimated supercapacitor peak SPs between a conservative 6 kW/kg and an aggressive 10 kW/kg. Beyond the aggressive estimates, an increase in SE or SP was found to have limited vehicle level benefits for a mild hybrid configuration, due to the diminishing returns associated with decreasing the relatively small ESS weight. Supercapacitors are able to be cycled much more frequently than batteries and are able to be fully charged and discharged with little to no effect on longevity [23].

Inherently geared for the unique power requirement peaks in the mild hybrid ConOps, supercapacitors can be arranged in an HESS where they deliver bursts of extremely high power, with the battery used primarily for energy storage. An additional benefit from the HESS is that it allows the battery to discharge more consistently at its rated power level, and using the supercapacitor to satisfy transient high power outputs takes advantage of the supercapacitor's immunity to cyclic degradation. Irregular energy release during battery discharge can damage the health of a battery and is drastically reduced by coupling the system with a supercapacitor [23].

3. Flywheels

Flywheels are a mechanical energy storage method consisting of a vacuum-sealed, magnetically levitated spinning rotor made of ultra-high strength material and an electric motor capable of applying (and absorbing) torques from the rotor. The flywheel has unique advantages over traditional energy storage methods such as an ability to store large amounts of energy, rapidly discharge its entire energy content, and repeat this for millions of cycles [28]. Due to the system being entirely mechanical, flywheels also have low temperature sensitivity and low toxicity [22]. This also ensures flywheels do not face the same lifetime degradation concerns as chemical ESSs and can be mechanically repaired due to their modular structure [29]. An FESS has been successfully demonstrated with NASA Glenn Research Center's G2 flywheel experiment which featured a 60,000 RPM, non-cryogenic magnetically levitated, carbon fiber flywheel [29]. To reduce the risk of damage caused by a structural failure of the rotor, the flywheel is encased in a high-strength enclosure and mounted on a three-axis gimbal to isolate the flywheel momentum from aircraft controls [30]. For this study, we sized the flywheel to have dimensions proportional to the G2 flywheel with the added constraint that the entire flywheel plus enclosure must fit below the passenger cabin of the aircraft.

The SE of the flywheel system is determined primarily by the ratio of strength to density of the flywheel rotor material, with stronger materials able to withstand higher rotational forces and store more rotational kinetic energy. We modeled an FESS as a rotor, enclosure, and electric motor, with the energy content of the FESS determined by the properties of the rotor and the power output determined by the size of the electric motor. By modeling a series of FESSs, we developed trends in SE and SP for each technology level that could be used as inputs for the ESS sizing component. Currently, the SOA material which is strong but lightweight is carbon fiber with a tensile strength of 3.5 GPa, which we selected for our conservative technology estimate [31]. For the purposes of this study, the nominal and aggressive

projections were set to be 10 GPa and 20 GPa, determined by the examination of SOA and published laboratory data for a carbon nanotube material with an EIS of 2035 [22, 31]. Laboratories have demonstrated 66 GPa carbon nanotubes on a molecular level; however, real-world application of this degree of strength remains far off. The quantity of flywheel modules required is inversely related to the rotor material strength, ranging from eight carbon fiber (3.5 GPa) flywheels to two carbon nanotube (20 GPa) flywheels.

The advent of single-walled carbon nanotubes has the potential to revolutionize the way energy is stored, with a theoretical tensile yield strength as high as 200 GPa, which would be greater than any other known material [22, 27]. A flywheel with this material would be able to store six times the energy of the aggressively forecasted 20 GPa flywheel. With an SE this high, only ten flywheels are needed to provide the roughly 75,000 MJ of energy required to complete the entire 900 NM economic mission. Some studies predict a rapid increase in flywheel SE over time and that flywheel SE will surpass chemical batteries in 30 years [22].

G. Cost Analysis Method

Direct operating cost plus interest (DOC+I) was chosen as the economic figure of merit for this study. DOC+I is a comprehensive metric that captures all aircraft-driven investment cost as well as aircraft-driven operating costs; DOC+I improvements correspond directly to profit increases for airlines. DOC+I includes aircraft ownership costs (either leasing cost or depreciation), fuel/energy costs, maintenance costs, flight crew costs, insurance costs, and flight equipment financing cost (the "+I" in DOC+I). Often, insertion of a new technology results in a net change in DOC+I driven by (1) an improvement in efficiency which yields decreased fuel burn and fuel cost and (2) an increase in size and complexity, manifested as increased ownership, maintenance, and interest costs. If the net change in DOC+I due to inclusion of a new technology is negative (reduced cost), then it can be said that the "business case closes" for that technology from the airline perspective.

The mild hybrid cost analysis approach was based on a tool called the Probabilistic Technology Investment Ranking System (PTIRS) [32]. PTIRS is a business case model for evaluating emerging technologies in the context of commercial aircraft development, manufacturing, and operations. PTIRS provides a complete estimate of all elements of DOC+I, including ownership cost (leasing or depreciation or amortization of owned assets). Calculating ownership costs requires calculating investment costs, which consist of production cost as well as amortized development costs. PTIRS is a complete life cycle cost model that calculates development costs, production costs, and all elements of airline operating costs, both direct and indirect. The PTIRS design is streamlined to support quick turnaround analysis but is flexible to support more detailed analysis when time and information are available.

PTIRS produces credible results through the development of cost estimating relationships (CERs) that are calibrated to reproduce the historical acquisition costs of commercial aircraft and historical operating costs of modern airlines. Benchmarking analysis indicates that with appropriate economic adjustments, PTIRS reproduces published aircraft prices for single-aisle-class aircraft [33] to within 13% and publicly available airline operations costs [34] to within 1%.

Besides the traditional airframe and subsystem CERs which are hardwired to individual work breakdown structure (WBS) items, PTIRS includes a library of CERs that can be applied to new hardware and software assemblies to be added anywhere in the WBS. When implementation of EAP requires addition of hardware to the propulsion system that more closely resembles electrical system hardware, an Electrical System production CER can be selected from the CER library, and the cost results can be mapped to the Propulsion WBS item, which would be more appropriate than adding them to the Electrical System WBS item. Furthermore, the library includes CERs for technologies which are new to commercial aircraft. New CERs have been added to the PTIRS CER library to address high-voltage, high-power electric motor/generators, high energy capacity lithium-ion battery packs, and high power capacity supercapacitors.

III. Results

A. Parametric Trade on TEEM Efficiency Benefit

TEEM was the only mild hybrid technology applied for this trade. For this trade and subsequent trades in this study, an HESS consisting of batteries and supercapacitors was used which assumed a nominal technology level. The TEEM efficiency benefit was varied parametrically from 0 to 3%. Figure 2 shows the percent change in block fuel of the aircraft with respect to the conventional baseline as a function of TEEM efficiency increase. From this figure, the break-even TEEM efficiency increase is approximately 1%, which is shown with a red star. This is approaching the lower bound of the assumed TEEM efficiency boost, which gives credence to the idea that TEEM may provide vehicle

level performance benefits on its own and is therefore a worthwhile concept to pursue.

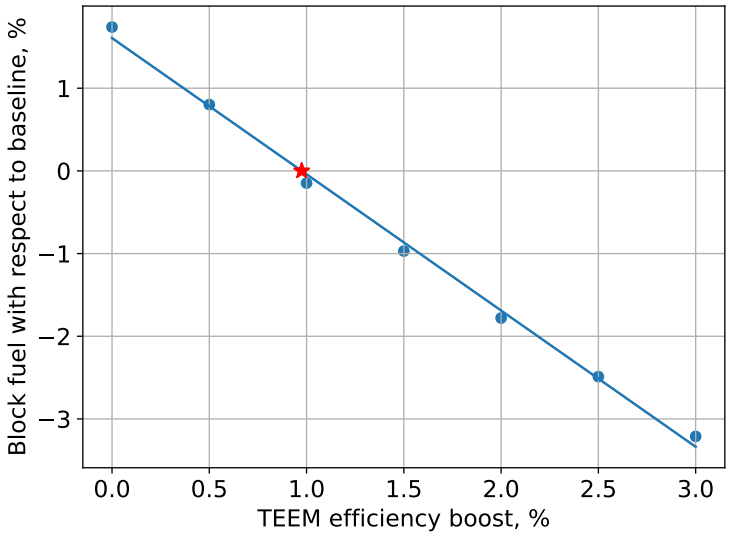

Fig. 2 Parametric trade on TEEM efficiency increase.

B. Impact of E-taxi, Electric Climb Assist, and Replacing APU

For this trade study, we examined the impact of incorporating TEEM, E-taxi, and electric climb assist onto the vehicle. Contours of percent change in block fuel with respect to the conventional baseline for varying climb assist power and TEEM efficiency boost are shown in Fig. 3. This trade revealed that an electric climb assist power of 400 kW maximized block fuel reduction for this configuration. The 400 kW LPS motors required for TEEM can be reused for the electric climb assist power requirements, up to their 400 kW rating. For electric climb assist powers greater than 400 kW, the LPS motors must be resized. The penalty of additional electrical component weight for larger LPS motors outweighs the benefits of more climb assist power.

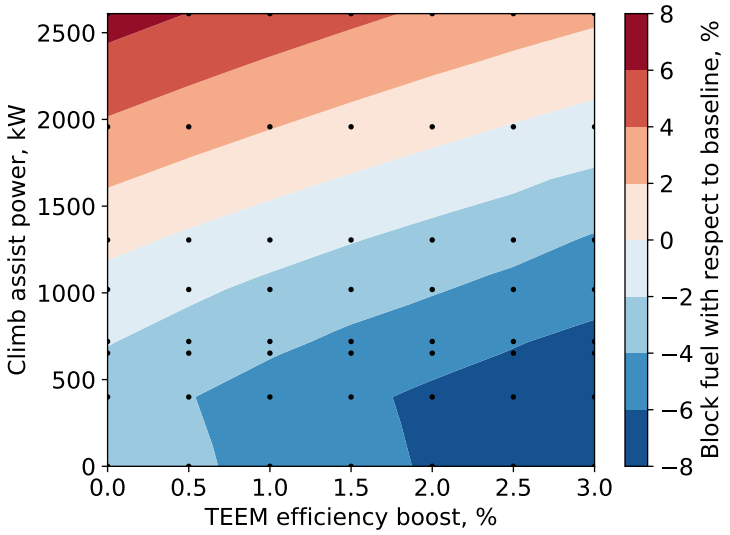

Fig. 3 Contours of percent change in block fuel with respect to the conventional baseline, for different climb assist and TEEM efficiency boost values.

Table 6 shows the block fuel results for different configurations featuring TEEM, E-taxi, electric climb assist, and replacing the APU. For the results in Table 6 and subsequent vehicle trades in this study, the efficiency increase due to TEEM was held fixed to a nominal 2%. For the economic mission, E-taxi provides a greater block fuel benefit on its own than TEEM on its own. Replacing the APU with ESS provides an additional 1.8% block fuel benefit to the mild hybrid configuration. The greatest block fuel benefit occurs when all four technologies are utilized; however, the additional benefit of implementing an electric climb assist is marginal.

Table 6 Block fuel benefits for different ConOps

Configuration	Block fuel, lb	Block fuel with respect to baseline
Conventional baseline	6,558	n/a
TEEM only	6,441	-1.8%
E-taxi only	6,292	-4.1%
TEEM and E-taxi	6,152	-6.2%
TEEM, E-taxi, and 400 kW climb assist	6,140	-6.4%
TEEM, E-taxi, 400 kW climb assist, and replacing APU	6,023	-8.2%

C. Impact of Energy Storage System Assumptions

The greatest penalty to aircraft performance for the mild hybrid configuration is the additional EAP component weight that is required. Because most of this weight comes from the ESS, the uncertainties in assumptions related to the ESS have a large impact on the uncertainty in block fuel benefits for the mild hybrid. To better quantify this uncertainty, the SE and SP assumptions were varied from conservative to aggressive for three ESS configurations: battery-only, battery and supercapacitor, and flywheel-only. The most promising mild hybrid configuration (TEEM, E-taxi, 400 kW climb assist, and replacing APU with ESS) was evaluated for each of these cases. Table 7 compares block fuel with respect to the conventional baseline for each case. Block fuel benefits are highly dependent on the ESS type chosen, with a battery and supercapacitor configuration showing the greatest benefits. The battery-only and flywheel-only cases have greater variation in block fuel benefits across technology level compared to the battery and supercapacitor case.

Table 7 Impact of ESS on block fuel benefits

	Block fuel with respect to baseline		
ESS configuration	Conservative	Nominal	Aggressive
Battery-only	-2.5%	-4.5%	-6.4%
Battery and supercapacitor	-7.1%	-8.2%	-9.0%
Flywheel-only	+8.6%	-5.7%	-8.3%

D. Final Configuration

The final mild hybrid configuration that we selected employs TEEM, E-taxi, a 400 kW climb assist, and replacing the APU with the ESS. For this configuration, the efficiency benefit due to TEEM was assumed to be 2%. The ESS is comprised of batteries and supercapacitors assuming a nominal technology level, with a 70-30 split between batteries and supercapacitors by weight. Table 8 compares this configuration with the conventional baseline in terms of important figures of merit. The mild hybrid carries around 4,500 lb of additional weight due to EAP components, including the electric powertrain and ESS. The percent difference in block fuel and CO_2e compared to the conventional baseline are -8.2% and -7.7%, respectively, for the economic mission. For the mild hybrid, the electric energy was less than 1% of the total energy (fuel plus electricity) used to complete the economic mission, with the mild hybrid consuming less total energy (-7.5%) than the conventional baseline.

Table 8 Comparison between conventional baseline and mild hybrid for economic mission

	Weight, lb		
Parameter	Baseline	Mild Hybrid	Percent Difference
Gross takeoff weight	111,023	114,874	+3.5%
Empty weight	66,587	70,874	+6.4%
Electric powertrain	0	1,598	n/a
Energy storage system	0	2,896	n/a
Block fuel	6,558	6,023	-8.2%
CO_2e	24,675	22,763	-7.7%

E. Cost Analysis

Cost analysis results comparing the mild hybrid and the conventional baseline for the 900 NM economic mission are shown in Fig. 4. As can be seen in the upper-right corner of the figure, the predicted cost impact of the mild hybrid technologies is a reduction in DOC+I per seat-mile of roughly $0.0005 USD per seat-mile at the 50th percentile confidence level. Although this is a very modest cost reduction, it comes with an 8% improvement in overall energy efficiency as shown in "Seat-mile per equivalent kWh" in the "Comparative Values" portion of the figure on the lower left. The fact that these technologies achieve a significant reduction in fuel burn and associated greenhouse gasses while lowering operating costs is a very favorable result.

The "Direct Operating Cost Impact" graph on the left of Fig. 4 shows that the estimated probability of achieving a reduction in operating cost is 85%, meaning there is a 15% chance that the inclusion of the technologies results in an increase in operating cost. There is a 98% chance that the potential cost benefit will fall between a reduction of $0.003 USD per seat-mile and an increase of $0.001 USD per seat-mile. The "Specific Cost Impacts" graph on the right of the figure shows the components of cost impact. It is expected that a significant decrease in fuel cost represented by the long blue bar will outweigh the addition of ground electricity cost plus the combined increases in ownership and maintenance costs due to a heavier and more complex aircraft.

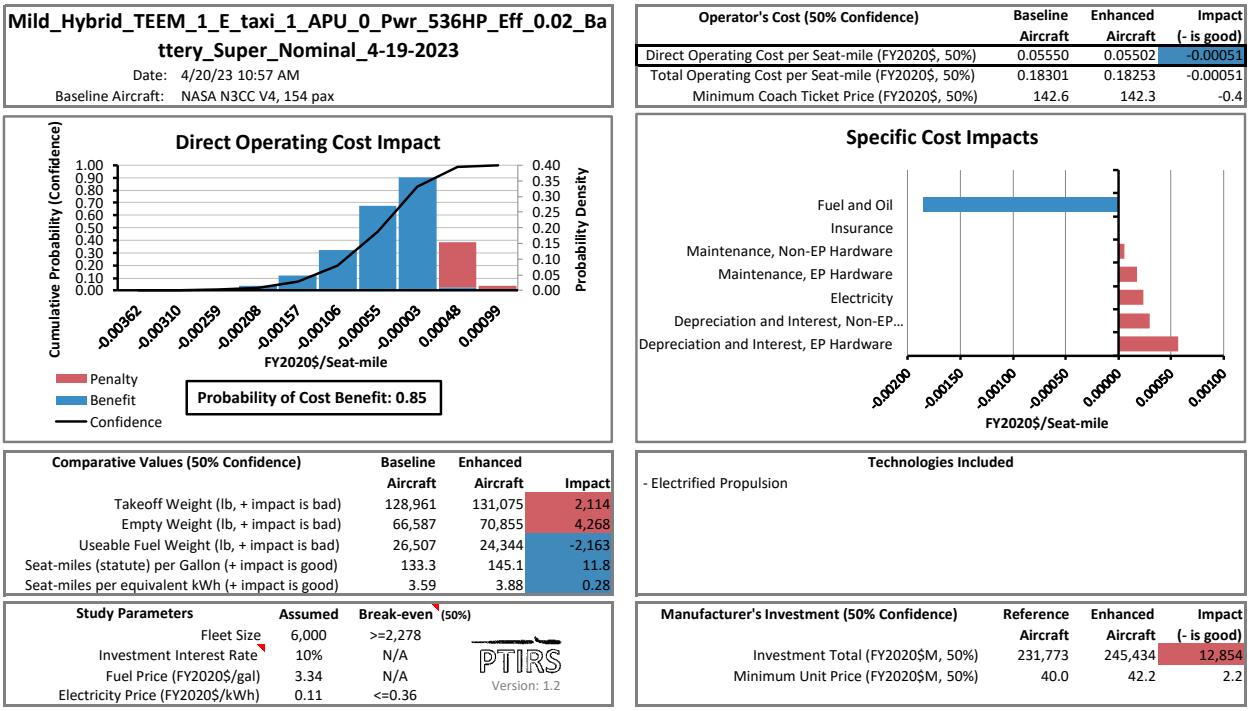

Operator's Cost (50% Confidence)	Baseline Aircraft	Enhanced Aircraft	Impact (- is good)
Direct Operating Cost per Seat-mile (FY2020$, 50%)	0.05550	0.05502	-0.00051
Total Operating Cost per Seat-mile (FY2020$, 50%)	0.18301	0.18253	-0.00051
Minimum Coach Ticket Price (FY2020$, 50%)	142.6	142.3	-0.4

Comparative Values (50% Confidence)	Baseline Aircraft	Enhanced Aircraft	Impact
Takeoff Weight (lb, + impact is bad)	128,961	131,075	2,114
Empty Weight (lb, + impact is bad)	66,587	70,855	4,268
Useable Fuel Weight (lb, + impact is bad)	26,507	24,344	-2,163
Seat-miles (statute) per Gallon (+ impact is good)	133.3	145.1	11.8
Seat-miles per equivalent kWh (+ impact is good)	3.59	3.88	0.28

Study Parameters	Assumed	Break-even (50%)
Fleet Size	6,000	>=2,278
Investment Interest Rate	10%	N/A
Fuel Price (FY2020$/gal)	3.34	N/A
Electricity Price (FY2020$/kWh)	0.11	<=0.36

Manufacturer's Investment (50% Confidence)	Reference Aircraft	Enhanced Aircraft	Impact (- is good)
Investment Total (FY2020$M, 50%)	231,773	245,434	12,854
Minimum Unit Price (FY2020$M, 50%)	40.0	42.2	2.2

Fig. 4 PTIRS cost analysis results of mild hybrid compared to conventional baseline. The mild hybrid is the "Enhanced Aircraft," and the conventional baseline is the "Baseline Aircraft."

IV. Concluding Remarks

This study investigated the implications of adopting a mild hybrid EAP approach to a single-aisle aircraft. We found that individual technologies (such as TEEM or E-taxi) were far less attractive on their own than when technologies were combined, with the best configuration making use of all of the technologies studied. There was significant synergy from using the ESS and electric motors integrated into the gas turbine for multiple applications, reducing the total electric component weight needed for implementation. We observed significant block fuel (-8.2%) and CO_2e (-7.7%) benefits compared to the conventional baseline, with only a modest increase in gross takeoff weight (+3.5%) due to added EAP components.

The prospect of lower emissions with a reduction (or at least a break-even) in DOC+I is a very strong incentive for airlines to adopt a mild hybrid configuration. The aviation industry is under increasing pressure from the public to reduce emissions, with additional government regulation and/or incentives for emissions reduction anticipated in the future. Previous NASA concepts that featured high levels of hybridization reduced emissions albeit with a significant cost penalty due to large batteries and higher empty weight. The mild hybrid configuration represents a viable path for emissions reduction without steep cost penalties or requiring the adoption of high risk technologies.

In future work, the methods developed for this study, such as ESS sizing and E-taxi modeling, will be adapted for use in the model-based systems analysis and engineering (MBSA&E) effort within NASA's AATT project. Further, a mild hybrid version of the Transonic Truss-Braced Wing (TTBW) aircraft concept will be developed to explore the potential benefits for the TTBW.

Acknowledgments

The NASA Advanced Air Transport Technology (AATT) project funded this research. The authors thank Jesse Quinlan, Eric Hendricks, Ty Marien, Jason Kirk, and Mark Guynn for their guidance and input. We also thank Michael Tong for his help with the gas turbine weight analysis in WATE++ and Jonathan Kratz for his help with dynamic engine analysis.

References

[1] Holladay, J., Abdullah, Z., and Heyne, J., "Sustainable Aviation Fuel: Review of Technical Pathways," DOE/EE-2041 8292, U.S. Department of Energy, 2020. URL https:/doi.org/10.2172/1660415, [retrieved 25 April 2023].

[2] U.S. Department of Energy, and National Aeronautics and Space Administration, "Joint Assessment of the RD Needs for Electric Aviation," 2021. URL https://www.anl.gov/article/white-paper-assessment-of-the-rd-needs-for-electric-aviation, [retrieved 25 April 2023].

[3] Kratz, J. L., Culley, D. E., and Thomas, G. L., "A Control Strategy for Turbine Electrified Energy Management," NASA/TM-2019-220353, 2019. URL https://ntrs.nasa.gov/citations/20190032490.

[4] Marien, T. V., Blaesser, N. J., Frederick, Z. J., Guynn, M. D., Kirk, J. T., Fisher, K., Schneider, S., Thacker, R. P., and Frederic, P., "Methdology Used for an Electrified Aircraft Propulsion Design Exploration," AIAA 2021-3191, 2021. URL https:/doi.org/10.2514/6.2021-3191.

[5] McCullers, L. A., "Aircraft Configuration Optimization Including Optimized Flight Profiles," *NASA Langley Research Center Recent Experiences in Multidisciplinary Analysis and Optimization, Part 1*, NASA, 1984, pp. 395–413. URL https://ntrs.nasa.gov/citations/19870002310.

[6] Gloudemans, J., Davis, P., and Gelhausen, P., "A Rapid Geometry Modeler for Conceptual Aircraft," AIAA 96-0052, 1996. URL https:/doi.org/10.2514/6.1996-52.

[7] Jones, S., "An Introduction to Thermodynamic Performance Analysis of Gas Turbine Engine Cycles Using the Numerical Propulsion System Simulation Code, Computing Systems in Engineering," NASA/TM–2007-214690, 2007. URL https://ntrs.nasa.gov/citations/20070018165.

[8] Tong, M. T., and Naylor, B. A., "An Object-Oriented Computer Code for Aircraft Engine Weight Estimation," NASA/TM 2009-219501, 2009. URL https://ntrs.nasa.gov/citations/20100000016.

[9] Boeing Commercial Airplanes, "737 Airplane Characteristics for Airport Planning," Airport Planning Manual D6-58325-6 Rev C, The Boeing Company, Oct. 2021. URL https://www.boeing.com/commercial/airports/plan_manuals.page.

[10] Camilleri, R., and Batra, A., "Assessing the environmental impact of aircraft taxiing technologies," *32nd Congress of the International Council of the Aeronautical Sciences*, ICAO, 2021. URL https://www.icas.org/ICAS_ARCHIVE/ICAS2020/data/preview/ICAS2020_1162.htm.

[11] Re, F., "Model-based Optimization, Control and Assessment of Electric Aircraft Taxi Systems," Ph.D. thesis, Technische Universität Darmstadt, Darmstadt, Germany, Jun. 2017. URL https://tuprints.ulb.tu-darmstadt.de/id/eprint/6239.

[12] Chakraborty, I., LeVine, M. J., Hassan, M., and Mavris, D. N., "Assessing Taxiing Trade Spaces from Aircraft, Airport, and Airline Perspectives," AIAA 2015-2386, 2015. URL https:/doi.org/10.2514/6.2015-2386.

[13] Daidzic, N. E., "Determination of Taxiing Resistances for Transport Category Airplane Tractive Propulsion," *Advances in Aircraft and Spacecraft Science*, Vol. 4, No. 6, 2017, pp. 651–677. URL https:/doi.org/10.12989/aas.2017.4.6.651, [retrieved 25 April 2023].

[14] Federal Aviation Administration, "Aviation System Performance Metrics (ASPM)," Online, Mar. 2023. URL https://aspm.faa.gov/, [retrieved 25 April 2023].

[15] Stockford, J. A., Lawson, C., and Liu, Z., "Benefit and Performance Impact Analysis of Using Hydrogen Fuel Cell Powered E-Taxi System on A320 Class Airliner," *The Aeronautical Journal*, Vol. 123, No. 1261, 2019, pp. 378–397. URL https://doi.org/10.1017/aer.2018.156, [retrieved 25 April 2023].

[16] Keçeci, M., Colpan, C. O., and Karakoç, T. H., "Reducing the Fuel Consumption and Emissions With the Use of an External Fuel Cell Hybrid Power Unit for Electric Taxiing at Airports," *International Journal of Hydrogen Energy*, 2021. URL https://doi.org/10.1016/j.ijhydene.2022.04.279, [retrieved 25 April 2023].

[17] Lukic, M., Giangrande, P., Hebala, A., Nuzzo, S., and Galea, M., "Review, Challenges, and Future Developments of Electric Taxiing Systems," *IEEE Transactions on Transportation Electrification*, Vol. 5, IEEE, 2019, pp. 1441–1457. URL https://doi.org/10.1109/tte.2019.2956862.

[18] Ehsani, M., Gao, Y., Longo, S., and Ebrahimi, K., *Modern Electric, Hybrid Electric, and Fuel Cell Vehicles*, 3rd ed., CRC Press, Boca Raton, FL, USA, 2018. URL https://doi.org/10.1201/9780429504884.

[19] Gao, Q., Tian, X., Tian, M., Yang, J., Zhang, J., and Lu, N., "An Engineering Calculation Method for Regenerative Braking Energy of Metro Vehicles," *IOP Conference Series: Materials Science and Engineering*, Vol. 569, No. 5, 2019, p. 052105. URL https://doi.org/10.1088/1757-899x/569/5/052105, [retrieved 25 April 2023].

[20] Tiede, B., O'Meara, C., and Jansen, R., "Battery Key Performance Projections Based on Historical Trends and Chemistries," *2022 IEEE Transportation Electrification Conference Expo (ITEC)*, IEEE, Anaheim, CA, USA, 2022, pp. 754–759. URL https://doi.org/10.1109/ITEC53557.2022.9814008.

[21] Kirk, J., Frederick, Z. J., Guynn, M. D., Blaesser, N. J., Phillips, B. D., Fisher, K., Schneider, S. J., and Frederic, P., "Continued Exploration of the Electrified Aircraft Propulsion Design Space," AIAA 2023-1354, 2023. URL https://doi.org/10.2514/6.2023-1354.

[22] Dever, T., Duffy, K., Provenza, A., Loyselle, P., Choi, B., Morrison, C., and Lowe, A., "Assessment of Technologies for Noncryogenic Hybrid Electric Propulsion," NASA/TP-2015-216588, 2015. URL https://ntrs.nasa.gov/citations/20150000747.

[23] Kouchachvili, L., Yaïci, W., and Entchev, E., "Hybrid Battery/Supercapacitor Energy Storage System for the Electric Vehicles," *Journal of Power Sources*, Vol. 374, 2018, pp. 237–248. URL https://doi.org/10.1016/j.jpowsour.2017.11.040, [retrieved 25 April 2023].

[24] Aravindan, V., Gnanaraj, J., Lee, Y.-S., and Madhavi, S., "Insertion-Type Electrodes for Nonaqueous Li-Ion Capacitors," *Chemical Reviews*, Vol. 114, American Chemical Society, 2014, pp. 11619–11635. URL https://doi.org/10.1021/cr5000915.

[25] Abraham, K. M., "Rechargeable Batteries for the 300-Mile Electric Vehicle and Beyond," *ECS Transactions*, Vol. 41, No. 31, 2012, pp. 27–34. URL https://doi.org/10.1149/1.3702853, [retrieved 25 April 2023].

[26] Velasco, A., Ryu, Y. K., Boscá, A., Ladrón-de Guevara, A., Hunt, E., Zuo, J., Pedrós, J., Calle, F., and Martinez, J., "Recent Trends in Graphene Supercapacitors: From Large Area to Microsupercapacitors," *Sustainable Energy Fuels*, Vol. 5, 2021, pp. 1235–1254. URL https://doi.org/10.1039/D0SE01849J, [retrieved 25 April 2023].

[27] Takakura, A., Beppu, K., Nishihara, T., Fukui, A., Kozeki, T., Namazu, T., Miyauchi, Y., and Itami, K., "Strength of Carbon Nanotubes Depends on their Chemical Structures," *Nature Communications*, Vol. 10, No. 3040, 2019. URL https://doi.org/10.1038/s41467-019-10959-7, [retrieved 25 April 2023].

[28] Olabi, A. G., Wilberforce, T., Abdelkareem, M. A., and Ramadan, M., "Critical Review of Flywheel Energy Storage System," *Energies*, Vol. 14, No. 8, 2021, p. 2159. URL https://doi.org/10.3390/en14082159, [retrieved 25 April 2023].

[29] Jansen, R., and Dever, T., "G2 Flywheel Module Design," AIAA 2004-5603, 2004. URL https://doi.org/10.2514/6.2004-5603.

[30] Dagnaes-Hansen, N. A., and Santos, I. F., "Magnetically Suspended Flywheel in Gimbal Mount - Test Bench Design and Experimental Validation," *Journal of Sound and Vibration*, Vol. 448, 2019, pp. 197–210. URL https://doi.org/10.1016/j.jsv.2019.01.023, [retrieved 25 April 2023].

[31] Toray Carbon Fibers America, Inc., "T1000G DATA SHEET No. CFA-008," Online, Oct. 2022. URL https://fileserver.mates.it/Prodotti/1_Rinforzi/TDS/Carbonio/Fibre/T1000G_DS.pdf, [retrieved 25 April 2023].

[32] Frederic, P., Bezos-O'Conner, G. M., and Nickol, C., "Cost Analysis Approach in the Development of Advanced Technologies for Green Aviation Aircraft," *Encyclopedia of Aerospace Engineering*, John Wiley & Sons, Ltd., 2016. URL https://doi.org/10.1002/9780470686652.eae1078.

[33] The Boeing Company, "About Boeing Commerical Airplanes," Online, 1998-2012. URL https://www.boeing.com/company/about-bca, [retrieved 25 April 2023].

[34] United States Department of Transportation, "Air Carrier Financial Reports (Form 41 Financial Data)," Online, Apr. 2020. URL https://www.transtats.bts.gov/, [retrieved 25 April 2023].